Journal of Informatics and Web Engineering
Vol. 5 No. 1 (February 2026) eISSN: 2821-370X

An Enhanced Glowworm Swarm Optimization for Minimizing Surface Roughness in Die Sinking Electrical Discharge Machining

Nurezayana Zainal[1*], Muhammad Ammar S.M. Shahrom[2], Mohamad Firdaus Ab. Aziz[3], Salama A. Mostafa[4], Anis Farhan Kamaruzzaman[5], Nor Bakiah Abd. Warif[6]**

[1,3,6]Faculty of Computer Science and Information Technology, Universiti Tun Hussein Onn Malaysia, 86400, Batu Pahat, Malaysia

[2]ZEN Computer Systems Sdn Bhd, 4808-1-28, CBD Perdana 2, Persiaran Flora, Cyberjaya, 63000 Cyberjaya, Malaysia

[4]Department of Artificial Intelligence Engineering Techniques, College of Technical Engineering, Al-noor University, Mosul 41012, Nineveh, Iraq

[5]Faculty of Computing, Universiti Teknologi Malaysia, 81310, Skudai, Johor, Malaysia

**corresponding author: (nurezayana@uthm.edu.my; ORCiD: 0000-0002-5424-8410)*

***corresponding author: (salama.adrees@alnoor.edu.iq; ORCiD: 0000-0001-5348-502X)*

Abstract - Electric Discharge Machining (EDM) is a non-traditional machining process that utilizes electric sparks between an electrode and a workpiece submerged in a dielectric fluid to ablate a material. It is commonly used in die-making, aerospace, automotive manufacturing, and medical manufacturing, because it can machine hard and complex materials with high precision. In this work, a Surface Roughness Optimization for EDM (SRO-EDM) model is proposed to investigate the machining performance of the die-sinking EDM process of titanium alloys. A regression-based combined approach of Glowworm Swarm Optimization (GSO) and a Two-Factor Interaction (2FI) model has been proposed to investigate the impact of four key process variables, namely voltage (V), peak current (Ip), pulse-on time (ton), and pulse-off time (toff) on surface roughness (Ra) at various locations on work surfaces. A Central Composite Design (CCD) was applied to systematically investigate parameter combinations. Statistical analysis was performed using analysis of variance (ANOVA), which confirmed the statistical significance of the selected parameters, and 2FI regression ($R^2 = 0.60$) with moderate-fit predictive accuracy was established. To enhance the quality of optimization, the Enhanced Glowworm Swarm Optimization (EGSO) algorithm is proposed by hybridizing the GSO with Artificial Fish Swarm (AFS) algorithm. The AFS module improves the exploration capability of the GSO and alleviates the local optima problem. For the experimental validation of the model, Response Surface Methodology (RSM) was used to generate the regression based on the developed model and as an objective function for optimization. Experimental results show that EGSO outperforms GSO in performance to achieve an optimized Ra (6.09 μm) compared to 6.106 μm through conventional GSO. The results demonstrate that the EGSO model can improve convergence accuracy and speed and is a practical method for EDM surface quality optimization in the high-precision manufacturing industry.

Keywords—Artificial Fish Swarm, Die-Sinking Electrical Discharge Machining, Enhanced Glowworm Swarm Optimization, Metaheuristic Optimization, Surface Roughness, Titanium Alloy, Two-Factor Interaction Regression Model

Received: 19 September 2025; Accepted: 25 November 2025; Published: 16 February 2026

1. INTRODUCTION

Machining processes are broadly categorized into traditional and nontraditional methods. These processes generally involve the use of workpieces, machine tools, and cutting instruments. Non-traditional machining techniques remove materials using electrical, thermal, chemical, or mechanical energy sources[1]. Among these, Electrical Discharge Machining (EDM) has emerged as one of the most widely adopted techniques owing to its ability to machine hard and geometrically complex materials that are difficult to process using conventional methods[2]. Unlike conventional machining processes, EDM can fabricate complex geometrical features with high precision and is applicable in the aerospace, automotive, and medical device industries[3], [4]. The process is based on controlled electrical discharges that are produced between a tool electrode and conductive workpiece, leading to localized melting and material removal[5]. Each shot in the discharge creates plasma temperatures in the range of 10–20 k°C that vaporize and evacuate material from the surface of the target[6], [7], [8]. It is important to optimize the EDM process, particularly in the case of die-sink EDM, to attain high precision and better surface finish, along with an enhanced material removal rate. This type of optimization for cost-effectiveness and sustainability is useful for reducing tool wear, increasing energy efficiency, and improving process stability[9]. However, EDM is a non-linear and multiparameter optimization problem; thus, existing optimization methods are confrontational challenges in terms of locating suitable global optima. To address this, Swarm Intelligence (SI) algorithms, which are based on the collective behaviour of organisms in nature, have emerged as effective meta-heuristics for solving complex optimization problems[3], [4], [10]. The aim of this research is to propose an improved EDM by enhancing the GSO algorithm with the objective function for the optimization of Ra in terms of the 2FI regression model.

The rest of this paper is organized as follows: In Section 2, related works and background algorithms are reviewed; the EGSO approach and modelling are described in Section 3; Section 4 provides results comparing EGSO with the standard GSO; and finally, conclusions and suggestions for further study are presented in Section 5.

2. LITERATURE REVIEW

2.1 Optimization and Swarm Intelligence (SI)

Optimization is an important tool in engineering[11], finance, [12] and data analysis[13]. Gradient-based methods are incapable of shifting perpendicular to the gradients in a high-dimensional or non-linear search space. In contrast, SI algorithms tend to draw inspiration from collective biological behaviour and implement decentralized and dynamic search strategies[14]. Examples include Ant Colony Optimization (ACO) [15] and artificial bee colonies (ABC)[16], which are inspired by the success of social insects in solving problems cooperatively through interaction and feedback mechanisms.

2.2 Glowworm Swarm Optimization (GSO)

The concept proposed by ACO was extended by Krishnan and Ghose [17] in their GSO algorithm for continuous optimization problems. In GSO, every agent (glowworm) contains luciferin intensity that is proportional to the fitness of the individual and moves towards its brighter neighbours. The algorithm repeats the luciferin update, movement, and decision range adjustment phases. Although GSO performs well as a global search algorithm, it has weaknesses in terms of slow distribution convergence and poor effective range-finding[18].

2.3 Hybrid and Improved GSO Models

Several augmented derivates of the Simple GSO (SGSO) have been proposed because of their inherent limitations, including slow convergence and early stagnation. Zhou et al. [19] introduced a hybrid glowworm swarm optimization (HGSO) that combines AFS and differential evolution (DE) algorithms and adopts a two-population co-evolution strategy to deliver faster convergence speed and better computational accuracy for multimodal optimization tasks. Similarly, Karthikeyan et al. [20] proposed a hybrid model of GSO with Genetic Algorithm (GA) methodology for the enhancement and optimization of SVM parameters in diabetic retinopathy classification. The suggested GSO-GA approach showed better results than existing approaches in terms of sensitivity, accuracy, and specificity. In a separate study, Zhou et al. [21] introduced a combination of GSO for cloud task scheduling and showed that the convergence

rate and resource allocation performance in a cloud system were improved. Chen et al. [22] proposed a hybrid algorithm by combining GSO with a 2-opt local search to address the spherical TSP. The enhanced version of GSO achieved better route optimization performance and stability than the basic form of GSO. Tang et al. [23] proposed the particle-GSO (PGSO) algorithm, incorporating mutation and local search considering the PSO, to achieve a higher convergence rate, robustness, and computational filter accuracy for UCAV path planning. In addition, Alphonsa et al. [24] proposed a genetically modified GSO model for privacy-preserving cloud computing in healthcare that could improve the efficiency of analysis and protect users' sensitive medical records. In summary, this research proves that hybridization helps enhance the global search of GSO combined with other metaheuristic or evolutionary methods, accelerates convergence, and further improves its adaptability to different types of problems.

2.4 Research Gap and Motivation

Although much has been done on the development of hybrid versions of GSO, little is found in the literature concerning their applications to optimization problems, specifically in manufacturing process optimization such as EDM. Existing literature has focused on computational or classification tasks rather than machining performance, such as Ra or material removal rate. Therefore, this investigation presents an EGSO with a combined AFS approach for die-sinking EDM parameter optimization. We used the experimental data published in [25] as pilot data for the model validation. The 2FI regression model was used as the objective function, and Ra was chosen as the cutting performance index. The aims of this study were to

- accelerating the convergence speed and enhancing the optimal solution of GSO;
- compare EGSO with the standard GSO in EDM optimization; and
- determine the best cutting conditions with minimum Ra value.

3 **RESEARCH METHODOLOGY**

This section describes chronological research, which involves the design of the research as well as the collection and investigation of data[1], [9]. The proposed research pattern should be supplemented by references so that the explanation can be scientifically accepted. The experiments presented in this paper were used to establish the EGSO algorithm and based on the experimental data of the mathematical model, some parameters that influence the Ra value were found. Data analysis is used to inform feature patterns and parameter relationships that can aid in formulating appropriate optimization goals and constraints. The AFS algorithm was also investigated to embed its exploration into the GSO to enhance its search ability.

Its working methodology comprises four major stages, as shown in Figure 1: data definition, developing the EGSO algorithm, optimizing the EGSO algorithm using a mathematical model, and evaluating the results of EGSO and GSO. A recent literature review of the fundamental knowledge of GSO coupled with the AFS algorithm and optimization process is presented in this work. Related work is a necessary and essential study for this experiment, which enables us to grasp the historical development, concepts, and principles of the two algorithms. In addition, a study related to learning supports the pinpointing of research gaps and limitations of both algorithms. To resolve these limitations, this study designed the research objective and enhanced algorithms, built knowledge, benchmarked, received methodological guidance, formulated a theoretical foundation, and generated new insights to ensure that the enhanced GSO algorithm development process was novel, well-informed, and contributed to the progress of this study.

In the validation period, both EGSO and GSO were compared for their performance in improving Ra. Experimental data [25] were used as a benchmark; if the optimized Ra value was less than that of the reference, then we accepted the success of the proposed EGSO approach.

3.1 Experimental Data

The dataset used in this study was compiled in [25]. The experiments were performed using Grace Model D-6030S die-sinking EDM. The material of the workpiece was Ti-13Zr-13Nb titanium alloy, which is applicable to biomedicine and has high strength, and a graphite tool electrode (10 mm diameter) was used. The debris was cleaned from the

discharge zone and stable sparking conditions were established through an impulse-jet cleansing system using commercial-grade kerosene as the dielectric medium.

Zirconium (Zr), niobium (Nb), and titanium (Ti)-based alloys contain small amounts of nitrogen, oxygen, carbon, silicon, and iron as impurity elements. The general range of the chemical composition of the alloy is listed in Table 1.

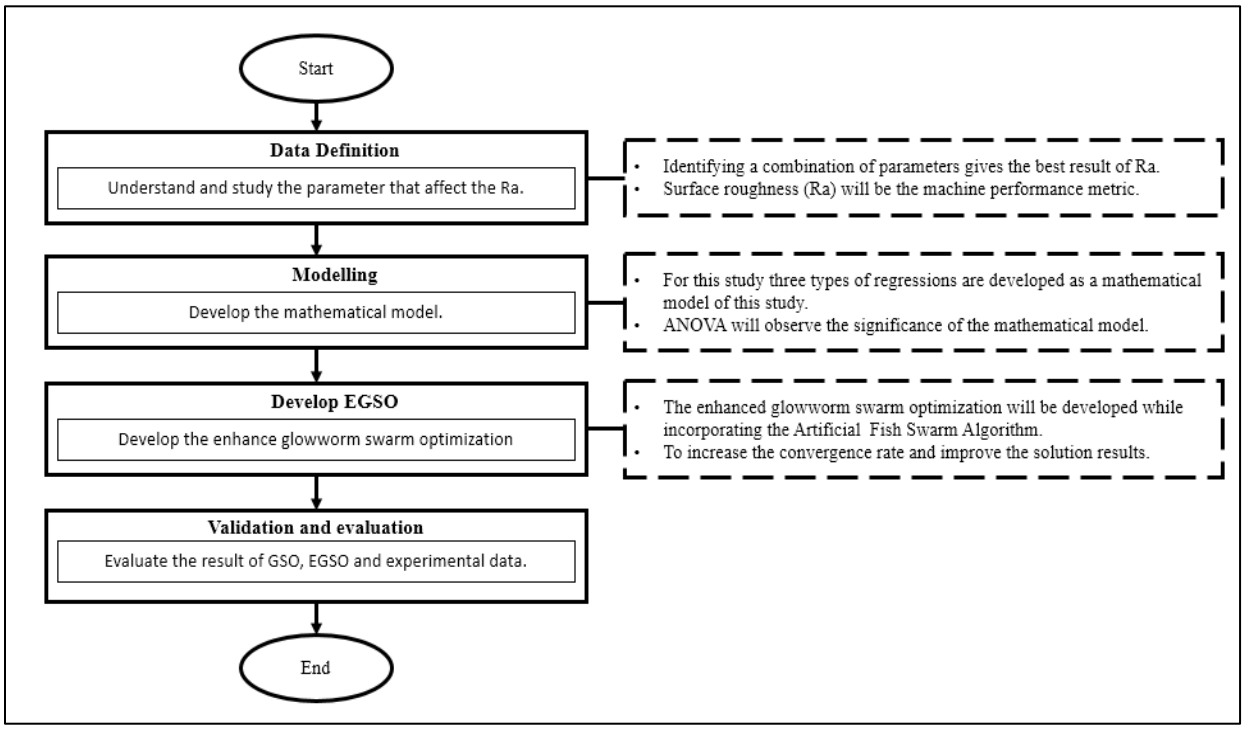

Figure 1. Operation Framework

Table 1. Chemical Composition of the Titanium Alloy (Ti–13Zr–13Nb) Used in the EDM Experiments

Elemental powder	**Impurity content (%)**				
	N	O	C	Si	Fe
Zr	0.080	0.450	0.028	-	0.030
Nb	0.038	0.620	0.020	-	0.040
Ti	0.872	0.349	0.073	0.025	0.040

The workpiece was 20 mm in diameter and 35 mm in length, and the machining area was 50 × 50 mm². The complete operating setup is presented in Table 2.

Table 2. The EDM Operating Conditions

Parameter	**Specification**
Machine	Grace D-6030S die-sinking EDM
Workpiece material	Ti-13Zr-13Nb titanium alloy
Working area	50 × 50 mm²
Workpiece size	20 mm (Ø) × 35 mm (length)
Dielectric fluid	Kerosene with impulse-jet cleansing
Electrode	Graphite (Ø 10 mm)

The design of the machining parameters, along with their respective units and levels, is summarized in Table 3.

Table 3. Experimental Factors and Their Corresponding Levels for EDM Processing of the Titanium Alloy

Parameter	Symbol	Unit	Level		
			1	2	3
Peak Current	Ip	A	8	12	16
Voltage	V	V	50	60	70
Pulse on time	Ton	µs	6	8	10
Pulse off time	Toff	µs	7	9	11

The experiments were designed using the RSM with a CCD to evaluate the effect of these four parameters on Ra. Thirty experimental runs were conducted, incorporating full factorial, star, and centre points. The resulting Ra values reported by Zubar et al. (2019) [21] ranged between 6.245 µm and 18.214 µm, with the lowest value achieved at *(V = 50 V, Ip = 8 A, Ton = 6 µs, Toff = 11 µs)*.

To provide a concise overview of the input ranges and corresponding Ra responses used in this study, Table 4, adapted from, [25] summarizes the parameter limits, central levels, and the statistical range of the measured Ra values. These summarized data serve as benchmarks for subsequent model development and optimization.

Table 4. Summary of EDM Process Parameter Ranges and Ra Statistics

Parameter	Symbol	Unit	Range	Central Level	Response (Ra, µm)
Voltage	V	V	50 – 70	60	6.245 – 18.214
Peak Current	Ip	A	8 – 16	12	—
Pulse On Time	Ton	µs	6 – 10	8	—
Pulse Off Time	Toff	µs	7 – 11	9	—

3.2 Mathematical Model

Optimization of the ideal Ra effect for the signal responses was achieved by a 2FI regression model according to Equation (1). This is the objective function used for the GSO and EGSO-AFS algorithms. The 2FI model was formulated as shown in Equation (1). In Equation (1), Ra is the surface roughness (µm), V stands for the servo voltage (V), Ip is a peak current (A), Ton and $Toff$ are pulse-on time and pulse-off time (µs), respectively. A 2FI model was established based on the experimental results (Table 4). The experimental data were analysed using Design Expert 13 (Statistical Software) to develop the 2FI model to represent the main effect and interaction of operation parameters on Ra. According to the R-squared (R^2) value derived from ANOVA, the 2FI model demonstrated the strongest relationship between the model and dependent variable at 0.60. The 2FI model showed the strongest relationship between the model and the dependent variable.

$$Ra = -4.465 + 0.106 * V + 0.686 * Ip + 1.895 * Ton - 1.785 * Toff - 0.008 * V * Ip - 0.021 * V * Ton + 0.026 * V * Toff + 0.029 * Ip * Ton - 0.015 * Ip * Toff + 0.048 * Ton * Toff \quad (1)$$

Based on the pilot results reported in [21], Table 3 summarizes the experimental design and their lower (Level 1) and upper (Level 3) factor settings. Equations (2) – (5) show the minimum and maximum ranges of the four parameters in EDM for optimization.

$$50V \leq V \leq 70V \quad (2)$$
$$8A \leq Ip \leq 16A \quad (3)$$
$$6\mu s \leq Ton \leq 10\mu s \quad (4)$$
$$7\mu s \leq Toff \leq 11\mu s \quad (5)$$

3.3 GSO

Motivated by the behaviour of glowworms in nature, the GSO algorithm finds its roots where each glowworm is attracted towards others with higher brightness[26], [27], [28]. In this metaphor, each glowworm symbolizes a

hypothetical optimizer, and its brightness, luciferin, equals the quality of the solution represented by that glowworm. Glowworms communicate with each other in a dynamic local-only neighbourhood, which is characterized by the sensor range and decision range. Attractive by nature to move towards a brighter companion for mating or foraging, glowworms inevitably take another attractive individual as a goal tangling each other across their decision-making neighbourhood because of the typically low luciferin value assigned based on randomness within the search space. Each glowworm then determines its moving direction by considering the information in the local neighbourhood. This collective behaviour is simulated by the GSO algorithm, which consists of three major phases: (i) luciferin update, (ii) movement, and (iii) neighbourhood range update. To update the luciferin phase, each glowworm updates its luciferin level by increasing the value proportional to its current fitness and decreasing it by the decay factor (decay factor representing the natural fading of luminescence). The luciferin level of each glowworm was determined using (1), according to the proposed rules of[26], [27], [29] (see Equation (6)).

$$l_i(t) = (1-\rho)l_i(t-1) + yJ\big(x_i(t)\big) \tag{6}$$

where $l_i(t)$ denotes the luciferin level of glowworm i at time t, ρ is the luciferin decay rate 0<$\rho < 1$, y is the luciferin enhancement factor, and $J\big(x_i(t)\big)$ signifies the value of the objective function at agent i's position at time t. In the GSO, each Glowworm (i.e., an agent) moves towards its neighbouring agents with a higher luciferin. This simulates the fact that glowworms prefer luminescent entities. In this stage, every agent uses a probability-based motion to find and move towards a neighbour with a higher quantity of luciferin, such that it can lead the swarm towards a better fitness area in the search space.

$$N_i(t) = \{j : d_{ij}(t) < r_d^i(t); l_j(t) < l_j\} \tag{7}$$

Equation (7) defines the neighbourhood set of Glowworm i at time t. The term $d_{ij}(t)$ denotes the Euclidean distance between glowworms i and j at time t, and $r_d^i(t)$ represents the dynamic neighborhood range associated with glowworm i. This range is constrained by the sensor boundary such that $\big(0 < r_d^i < r_s^i\big)$. For each Glowworm i, the probability of movement towards a neighbouring glowworm j ∈ $N_i(t)$ is determined using Equation (8).

$$P_{ij}(\mathrm{t}) = \frac{l_j(t) - l_i(t)}{\sum_{k\in N_i(t)} l_k(t) - l_i(t)} \tag{8}$$

where j is a neighbor of the glowworm i. In the current iteration t, glowworm i chooses glowworm from its neighbours $N_i(t)$ using the Roulette Wheel method. Glowworms with higher probabilities are expected to be picked out from neighbouring groups. Then, during the movement phase of the glowworms, the position of the current glowworm was adjusted according to the position of the selected neighbour. This movement can be expressed as in Equation (9).

$$x_i(t+1) = x_i(t) + s\left[\frac{x_j(t) - x_i(t)}{\big||x_j(t) - x_i(t)|\big|}\right] \tag{9}$$

where s (> 0) represents the step size, || || is the Euclidean norm operator. Then, $x_i(t) \in R^m$ represents the location of glowworm i at time t in the m-dimensional real space R^m. $x_i(t)$ and $x_i(t+1)$ are the previous and new positions of the ith glowworm, respectively.

The last step in GSO is the neighbourhood range update phase, which is used to detect multiple peaks in a multimodal function landscape. Next, let r_0 be the initial neighborhood range value of each worm ($r_d^i(0) = r_0$, for all i). The following rule (Equation (10)) is used to adaptively update the neighbourhood range update rule for each glowworm.

$$r_d^i(t+1) = \min\big\{r_s, max\big\{0, r_d^i(t) + \beta(n_t - |N_i(t)|)\big\}\big\} \tag{10}$$

Here, β, r_s and n_t denote the constant radial sensor range, model constant, and constant controlling the neighbour count, respectively. Figure 2 illustrates the sensory and decision radii associated with glowworm i.

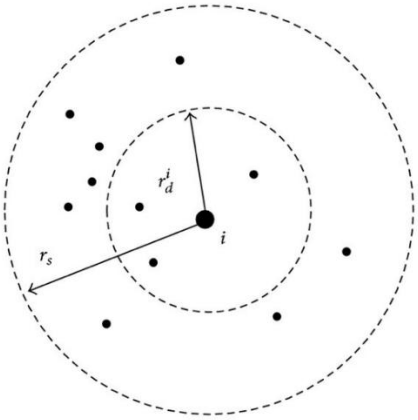

Figure 2. Sensory and Decision Radius of Glowworm i [22]

As depicted in Figure. 2, r_s is the sensor radius and r_d^i is the initial neighborhood range that is defined during the update of the neighborhood range. When Glowworm i moves, this process is repeated to find and reposition nearby glowworms in the sensing range.

3.4 *AFS Algorithm*

The AFS algorithm is a biologically motivated optimization algorithm that emulates how fish search for food in aquatic environments. It is also able to reach the global optimum as it mimics natural processes such as foraging, clustering, and the following of agents to reach global optima through a sequence of local interactions. The AFS algorithm The AFS is based on SI and models the collective motion of a group of fish to effectively solve difficult optimization problems [30 - 33]. Based on detailed observations of fish nature, AFS adopts a cooperative search method to achieve a trade-off between searching and optimizing in multidimensional solution spaces.

X_i is the current position of i and X_j is a random state within the field of view $rand()$ which generates a random number in [0, 1]. The distance between any two fish i and j is defined as $d_{ij} = ||X_i - X_j||$, where denotes the visual range of each fish. The parameter $trynumber$ denotes the number of trials when each fish attempts to search for a better location and δ is the crowding factor $(0 < \delta < 1)$. nf is the number of neighbouring fish that are within the visible distance $(d_{ij} < Visual)$, and $step$ represents how far AF moves. The set $T = \{X_j | ||X_i - X_j|| < Visual\}$ represents all the places that the i-th fish can visit with respect to its current visual range. The adaptive effects of these parameters are the foundation of the AFS behavioural model and allow each fish to assess an area of high potential versus other areas in the search space, moving towards improved points, as illustrated below.

Based on Equation (11), AF-Prey is the basic foraging mechanism for AF. Fish usually sense fluid cues in their visual fields and swim to regions where food concentrations are higher. Similarly, in the AFS algorithm, X_i is the current state of a fish and is randomly chosen to move into another state $X_j (X_j \in t)$ with its visual range. The variable y denotes the concentration of food in the spot. The larger the visual range, the easier it is for the algorithm to find regions with more food, thereby enhancing the global optimal solution and convergence speed of the algorithms. Mathematically, the behaviour of the prey was calculated as in Equation (11).

$$prey(X_i^{t+1}) = \begin{cases} X_i^t + \left(\dfrac{X_j - X_i^t}{||X_j - X_i^t||}\right).step.rand(), & y_j > y_i \\ X_i + (2.rand() - 1)step, & else \end{cases} \quad (11)$$

where $rand()$ yields values between zero and one. From Equation (12), it follows that AF-Swarm behaviour simulates fish collective movement as a means of survival and resistance against threats during migration. Denote X_i as the

present location of artificial fish and let $X_c = \sum_{xj \in S} Xj/nf$ are the central coordinates of the swarm, nf is the number of nearest neighbours in visual field $(d_{ij} < Visual)$, and n is a total number of fish in population. The mathematical representation of swarm behaviour is as follows.

$$swarm\ (X_i^{t+1}) = X_i^t + step.\frac{X_c - X_i}{||X_c - X_i||}, \text{if } \frac{y_c}{nf} > \delta y_i \tag{12}$$

Based on Equation (13), AF-Follow represents the attraction of a fish to other fish that find food patches. On the other hand, when several fish discover an area of high food concentration during movement, nearby prey is attracted to them to find the area faster. Let X_i be the current position of an artificial fish and let X_{max} state have a higher food concentration (higher fitness function value). The maximum food concentration was given by $y_{max} = \max\{f(X_j)|X_j \in t\}$. The positions of the fish are then updated by, as expressed in Equation (13).

$$follow(X_i^{t+1}) = \begin{cases} X_i^t + step\left(\frac{X_{max} - X_i}{||X_{max} - X_i||}\right), & \frac{y_{max}}{nf} > \delta y_i \\ prey(X_i), & else \end{cases} \tag{13}$$

3.5 Modelling the EGSO

The EGSO algorithm is a combination of GSO and AFS to enhance global searching capabilities and avoid local minima. EGSO is introduced to optimize Ra, which is a significant parameter for evaluating machining performance. In machining, Ra is used as a measure of the average Ra of a machined workpiece [25], with smaller values denoting smoother surfaces and improved machining precision. Thus, the ultimate purpose of EGSO in this context is to determine the local minimum value of Ra with better surface quality. The practical realization of EGSO starts with the initialization of the parameters. The settings of the parameters in this study were as follows:

- $n = 50$: Number of glowworms (population size).
- $max\_t = 100$: threshold for maximum iterations.
- $dim = 4$: Number of dimensions in the optimization problem (to be precisely associated with four EDM parameters).
- $s = 0.5$: This is the step size, and it specifies the movement that needs to be done per iteration.
- $\beta = 0.08$: Attractiveness coefficient that affects movement towards brighter glowworms.
- $\gamma = 0.6$ is the decay factor that controls the reduction of attractiveness with distance.
- $n_t = 5$: threshold for the neighbourhood used in the interaction area.
- $l_0 = 5$ is the initial neighbourhood radius.

These parameter settings enable EGSO to determine the optimal Ra value between exploration and exploitation. The complete EGSO algorithm was depicted to describe how the levels of luciferin were iteratively updated, the movement was adaptively responded to, and the decision range was modified (as shown in Figure 3). In the luciferin update process, each glowworm updates its light intensity based on its fitness results (brighter glowworms correspond to solutions of better quality and attract closer agents). During the movement phase, glowworms move to neighbours with a higher value of luciferin, and the movement is controlled by the reward factor and step size. Second, in the decision range update step, both ranges are adjusted to guarantee effective communication and convergence within the swarm.

Finally, EGSO also includes a random displacement technique in the prey stage, which reflects the movement of the AFS algorithm. During the random search phase, all virtual fish in the AFS model move randomly to traverse the search space for food, according to Equation (5). Likewise, in EGSO, each Glowworm can move randomly around its current position. By adding stochastic movement, this algorithm improves its capability to exit from local optima and search for novel regions of the solution space, resulting in an improvement in both the solution quality and speed of convergence.

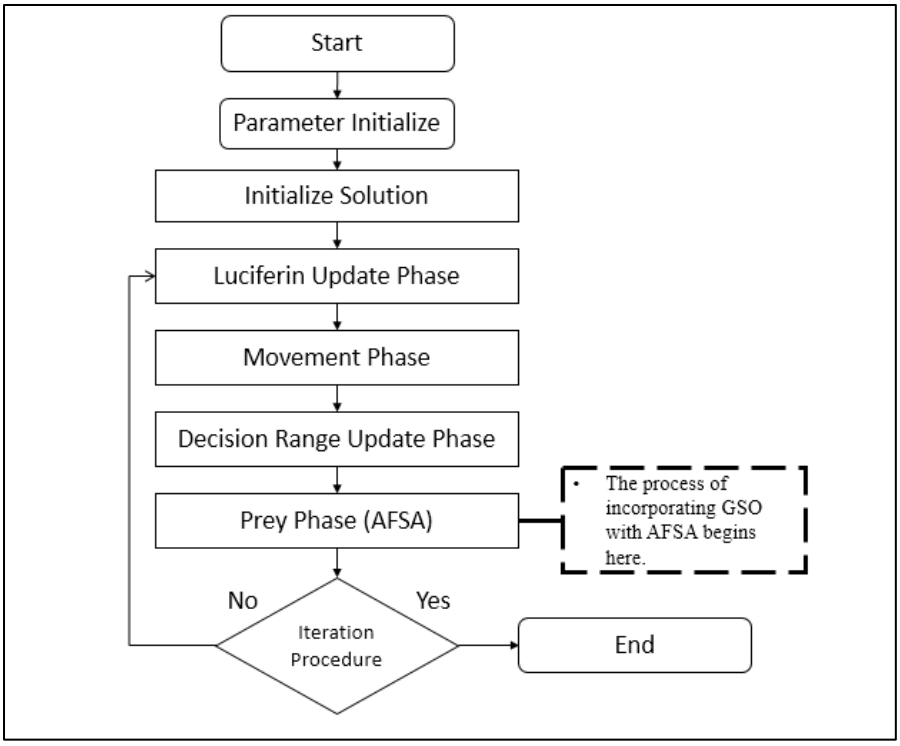

Figure 3. The Flowchart of the EGSO Model

4 RESULTS AND DISCUSSIONS

This section presents the solution quality and validation results for the EGSO and standard GSO models in comparison with experimental benchmark data. As listed in Table 4, the lowest Ra value obtained from the machining experiment by Zubar *et al.* [21] was 6.245 μm, corresponding to the parameter combination *(V = 50.000 V, Ip = 8.000 A, Ton = 6.000 µs, Toff = 11.000 µs)*. This experimental minimum was used as the benchmark to evaluate the optimization performance of both algorithms.

In optimization problems, an optimal solution refers to the best possible configuration that satisfies all problem constraints while minimizing or maximizing the objective function. The objective of this study is to obtain the minimum Ra value by comparing the EGSO and GSO algorithms. The results summarized in Table 5 show that EGSO achieved the lowest Ra value of 6.098 μm with the same parameter combination as the experimental benchmark, whereas GSO achieved a slightly higher value of 6.106 μm.

Table 5. Comparison of Results for EGSO, GSO, and Experimental Data

Item	Experimental Data	GSO	EGSO
Parameters	[50.000, 8.000, 6.000, 11.000]	[50.101, 8.052, 6.126, 11.000]	[50.000, 8.000, 6.000, 11.000]
Result (Ra µm)	6.245 µm	6.106 µm	6.098 µm

The GSO algorithm achieved an Ra value of 6.106 μm with a parameter combination *(50.101 V, 8.052 A, 6.126 µs, 11 µs)*. Both optimization algorithms produced lower Ra values compared to the experimental benchmark of 6.245 μm (Table 4), confirming their effectiveness in enhancing surface quality. However, the EGSO algorithm yielded the lowest Ra value of 6.098 μm, demonstrating its superior performance in achieving the optimal solution and validating its improved search capability over the standard GSO. Figure 4 shows the average fitness of an individual for EGSO and GSO for optimizing Ra.

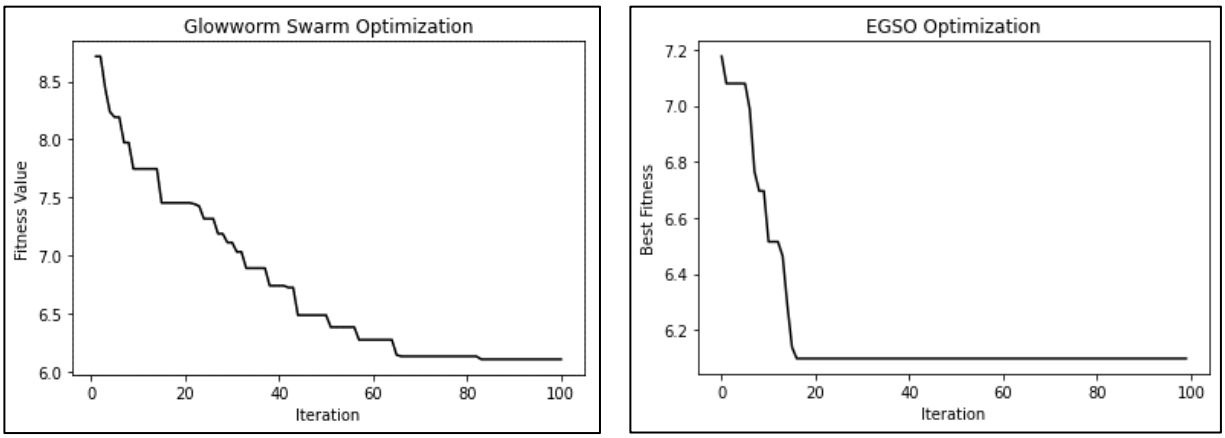

(a) GSO (b) EGSO

Figure 4. The Average Fitness of Individuals for GSO and EGSO in Optimized Ra

As shown in Figure 4, EGSO and GSO converge during the optimization process, and EGSO converges more quickly. The best Ra value of EGSO was achieved at the 31st iteration, and for GSO after the 83rd iteration. The rapid convergence, combined with a lower predicted Ra, highlights the EGSO's improved efficiency, stability, and effectiveness in optimizing the EDM process compared to the standard GSO. Thus, the rapid convergence and better Ra value obtained by EGSO emphasized its better optimization efficiency and stability than that of the standard GSO. Moreover, the superior performance of the EGSO algorithm can also be attributed to the following:

a. EGSO has an adaptive step size that is dynamically based on local fitness improvements, allowing faster convergence near the optimum.
b. EGSO improved the luciferin update mechanism, which led to better exploration of promising regions while avoiding premature convergence in local minima.
c. EGSO adaptively modifies the neighbourhood radius to balance exploration and exploitation and to improve stability and solution quality.

5 CONCLUSION

In this study, an EGSO model combining the AFS algorithm in the prey phase was proposed to determine the optimal parameters of the EDM process. The AFS integration enhances the search efficiency of the standard GSO by strengthening its exploration and preventing early convergence. Optimization was performed according to the constraints of a 2FI regression model, which served as the objective function for Ra. Statistical modelling with ANOVA showed that the 2FI model was significant, with a coefficient of determination R^2= 0.60, demonstrating its relevance in predictive terms. Numerical experiments indicate that EGSO is better than GSO in terms of both solution quality and convergence speed, achieving an Ra of 6.098 μm compared to GSO's 6.106 μm. This enhancement confirms the possibility of considering EGSO as a more open optimization platform for complex non-linear shape factors. However, its performance could be a problem domain and enhancement strategy dependent. Further research should be conducted to explore different hybridization techniques and evaluate the scalability and robustness of EGSO over wider optimization problems, especially in advanced manufacturing. In general, this work helps the study of SI in the sense that combining complementary algorithms can improve both the solution accuracy and adaptability in practical engineering.

ACKNOWLEDGEMENT

The authors would like to thank the anonymous reviewers for their suggestions on improving the paper.

FUNDING STATEMENT

This research was supported by the Ministry of Higher Education (MOHE) through the Fundamental Research Grant Scheme (FRGS/1/2021/ICT02/UTHM/03/1).

AUTHOR CONTRIBUTIONS

Nurezayana Zainal: Project Administration, Supervision, Validator, Writing – Review & Editing;
Muhammad Ammar S.M Shahrom: Conceptualization, Methodology, Writing – Original Draft Preparation;
Mohamad Firdaus Ab. Aziz: Project Administration, Supervision, Writing – Review & Editing;
Salama A. Mostafa: Project Administration, Writing – Review & Editing;
Anis Farhan Kamaruzzaman: Project Administration, Writing – Review & Editing;
Nor Bakiah Abd. Warif: Project Administration, Writing – Review & Editing.

CONFLICT OF INTERESTS

No conflict of interests were disclosed.

ETHICS STATEMENTS

Our publication ethics follow The Committee of Publication Ethics (COPE) guidelines. https://publicationethics.org/

DATA AVAILABILITY

The data that support the findings of this study are available from the corresponding author upon reasonable request.

REFERENCES

[1] W. Ming *et al.*, "Progress in non-traditional machining of amorphous alloys," *Ceram Int*, vol. 49, no. 2, pp. 1585–1604, Jan. 2023, doi: 10.1016/j.ceramint.2022.10.349.

[2] N. Zainal, A. Mohd Zain, S. Sharif, H. Nuzly Abdull Hamed, and S. Mohamad Yusuf, "An integrated study of surface roughness in EDM process using regression analysis and GSO algorithm," in *Journal of Physics: Conference Series*, Institute of Physics Publishing, Sep. 2017, doi: 10.1088/1742-6596/892/1/012002.

[3] Ajit, D. K. Bhalla, and S. Sundriyal, "A Comparative Study of Die-Sinking and Near-Dry EDM Using MADM-Based Parameter Optimization," *MAPAN*, Nov. 2025, doi: 10.1007/s12647-025-00864-4.

[4] M. P. Uddin, A. Majumder, J. D. Barma, and S. Mirjalili, "An Improved Multi-Objective Harris Hawks Optimization Algorithm for Solving EDM Problems," *Arab J Sci Eng*, vol. 50, no. 15, pp. 12403–12448, Aug. 2025, doi: 10.1007/s13369-024-09694-z.

[5] V. Choudhari *et al.*, "A Review on Electric Discharge Machining with Assisted Processes for Precise Machining of Hard to Cut Materials," 2026, pp. 700–712, doi: 10.1007/978-981-95-1750-3_80.

[6] P. Karmiris-Obratański, E. L. Papazoglou, B. Leszczyńska-Madej, K. Zagórski, and A. P. Markopoulos, "A comprehensive study on processing ti–6al–4v eli with high power edm," *Materials*, vol. 14, no. 2, pp. 1–17, Jan. 2021, doi: 10.3390/ma14020303.

[7] H. Sharma, and B. Singh, "Experimental design based optimization of process parameters for EDM of AA6068," *Mater Today Proc*, Feb. 2023, doi: 10.1016/j.matpr.2023.02.166.

[8] H. Sharma, and B. Singh, "Experimental design based optimization of process parameters for EDM of AA6068," *Mater Today Proc*, 2023, doi: 10.1016/j.matpr.2023.02.166.

[9] N. Zainal, A. Mohd Zain, and S. Sharif, "A study of electrode wear ratio on EDM of Ti-6AL-4V with copper-tungsten electrode," in *MATEC Web of Conferences*, 2016, doi: 10.1051/matecconf/20167801013.

[10] B. Gugulothu, "Optimization of process parameters on EDM of titanium alloy," in *Materials Today: Proceedings*, Elsevier Ltd, Jan. 2020, pp. 257–262, doi: 10.1016/j.matpr.2019.10.150.

[11] C. Qu, and W. He, "A Cuckoo Search Algorithm with Complex Local Search Method for Solving Engineering Structural Optimization Problem," *MATEC Web of Conferences*, vol. 40, p. 09009, Jan. 2016, doi: 10.1051/matecconf/20164009009.

[12] F. C. M. Ortiz, and C. J. Costa, "RPA in Finance: supporting portfolio management : Applying a software robot in a portfolio optimization problem," in *2020 15th Iberian Conference on Information Systems and Technologies (CISTI)*, IEEE, Jun. 2020, pp. 1–6, doi: 10.23919/CISTI49556.2020.9141155.

[13] M. AL-Alawi, Y. Mohamed, and A. Bouferguene, "Application of industrial pipelines data generator in the experimental analysis: Pipe spooling optimization problem definition, formulation, and testing," *Advanced Engineering Informatics*, vol. 43, p. 101007, Jan. 2020, doi: 10.1016/j.aei.2019.101007.

[14] R. Alizadehsani *et al.*, "Swarm Intelligence in Internet of Medical Things: A Review," *Sensors*, vol. 23, no. 3, p. 1466, Jan. 2023, doi: 10.3390/s23031466.

[15] S. Janakiraman, "A Hybrid Ant Colony and Artificial Bee Colony Optimization Algorithm-based Cluster Head Selection for IoT," *Procedia Comput Sci*, vol. 143, pp. 360–366, 2018, doi: 10.1016/j.procs.2018.10.407.

[16] C. B. Kalayci, A. Hancilar, A. Gungor, and S. M. Gupta, "Multi-objective fuzzy disassembly line balancing using a hybrid discrete artificial bee colony algorithm," *J Manuf Syst*, vol. 37, pp. 672–682, Oct. 2015, doi: 10.1016/j.jmsy.2014.11.015.

[17] A. Bassel, S. Adnan Abed, S. Abdullah, M. Jan Nordin, and A. Turky, "An Improved Glowworm Swarm Optimization Based on Various Mutation Operators," *IEEE Access*, vol. 12, pp. 106359–106384, 2024, doi: 10.1109/ACCESS.2024.3436899.

[18] C. B. Kalayci, A. Hancilar, A. Gungor, and S. M. Gupta, "Multi-objective fuzzy disassembly line balancing using a hybrid discrete artificial bee colony algorithm," *J Manuf Syst*, vol. 37, pp. 672–682, Oct. 2015, doi: 10.1016/j.jmsy.2014.11.015.

[19] Y. Zhou, G. Zhou, and J. Zhang, "A hybrid glowworm swarm optimization algorithm to solve constrained multimodal functions optimization," *Optimization*, vol. 64, no. 4, pp. 1057–1080, Apr. 2015, doi: 10.1080/02331934.2013.793329.

[20] R. Karthikeyan, and P. Alli, "Feature Selection and Parameters Optimization of Support Vector Machines Based on Hybrid Glowworm Swarm Optimization for Classification of Diabetic Retinopathy," *J Med Syst*, vol. 42, no. 10, p. 195, Oct. 2018, doi: 10.1007/s10916-018-1055-x.

[21] J. Zhou, and S. Dong, "Hybrid glowworm swarm optimization for task scheduling in the cloud environment," *Engineering Optimization*, vol. 50, no. 6, pp. 949–964, Jun. 2018, doi: 10.1080/0305215X.2017.1361418.

[22] X. Chen, Y. Zhou, Z. Tang, and Q. Luo, "A hybrid algorithm combining glowworm swarm optimization and complete 2-opt algorithm for spherical travelling salesman problems," *Appl Soft Comput*, vol. 58, pp. 104–114, Sep. 2017, doi: 10.1016/j.asoc.2017.04.057.

[23] Z. Tang, and Y. Zhou, "A Glowworm Swarm Optimization Algorithm for Uninhabited Combat Air Vehicle Path Planning," *Journal of Intelligent Systems*, vol. 24, no. 1, pp. 69–83, Mar. 2015, doi: 10.1515/jisys-2013-0066.

[24] M. M. Annie Alphonsa, and P. Amudhavalli, "Genetically modified glowworm swarm optimization based privacy preservation in cloud computing for healthcare sector," *Evol Intell*, vol. 11, no. 1–2, pp. 101–116, Oct. 2018, doi: 10.1007/s12065-018-0162-4.

[25] A. Soundhar, H. A. Zubar, M. T. B. H. H. Sultan, and J. Kandasamy, "Dataset on optimization of EDM machining parameters by using central composite design," *Data Brief*, vol. 23, p. 103671, Apr. 2019, doi: 10.1016/j.dib.2019.01.019.

[26] C. Sivamathi, G. S. Karthick, and S. Vijayarani, "Glowworm Swarm Optimization Algorithm for Retrieval of High Utility Itemsets," in *2024 International Conference on Smart Systems for Electrical, Electronics, Communication and Computer Engineering (ICSSEECC)*, IEEE, Jun. 2024, pp. 111–116. doi: 10.1109/ICSSEECC61126.2024.10649418.

[27] S. K. Suman, and O. P. Suman, "A Metaheuristic Mutation-Based Glowworm Swarm Optimization Model for Balancing Load in a Cloud Computational Environment," 2026, pp. 247–261. doi: 10.1007/978-981-96-7614-9_19.

[28] S. Perumal, J. Vijayaraj, and D. Prabakar, "Optimizing energy efficiency and coverage in wireless sensor networks using Delaunay Triangulation and glowworm swarm optimization," *Peer Peer Netw Appl*, vol. 18, no. 6, p. 318, Oct. 2025, doi: 10.1007/s12083-025-02103-8.

[29] I. Singh, H. Malhotra, Shruti, S. Jain, S. Kumar Jha, and Y. Kumar Pal, "Evolutionary Neuro-Fuzzy Network and Novel Hybrid Adaptive Crow Search-Modified Glowworm Swarm Optimization for Credit Card Fraud Detection," 2024, pp. 309–318. doi: 10.1007/978-3-031-70018-7_34.

[30] N. Zainal, A. M. Zain, and S. Sharif, "Overview of Artificial Fish Swarm Algorithm and its Applications in Industrial Problems," *Applied Mechanics and Materials*, vol. 815, pp. 253–257, Nov. 2015, doi: 10.4028/www.scientific.net/AMM.815.253.

[31] F. Pourpanah, R. Wang, C. P. Lim, X.-Z. Wang, and D. Yazdani, "A review of artificial fish swarm algorithms: recent advances and applications," *Artif Intell Rev*, vol. 56, no. 3, pp. 1867–1903, Mar. 2023, doi: 10.1007/s10462-022-10214-4.

[32] V. Kourepinis, C. Iliopoulou, I. Tassopoulos, and G. Beligiannis, "An artificial fish swarm optimization algorithm for the urban transit routing problem," *Appl Soft Comput*, vol. 155, p. 111446, Apr. 2024, doi: 10.1016/j.asoc.2024.111446.

[33] J. Han, J. Zhu, Y. Zhang, Z. Zhao, and Z. An, "Optimization of machining process route for internal joint parts using artificial fish swarm algorithm," *Journal of Advanced Mechanical Design, Systems, and Manufacturing*, vol. 19, no. 1, p. 2025jamdsm0009, 2025, doi: 10.1299/jamdsm.2025jamdsm0009.

BIOGRAPHIES OF AUTHORS

Nurezayana Zainal is a Senior Lecturer at the Faculty of Computer Science and Information Technology from Universiti Tun Hussein Onn Malaysia, Malaysia. She received her PhD in Computer Science from Universiti Teknologi Malaysia (UTM) in 2018 and her Master of Science (Computer Science) from the same university in 2014. Her research interests include soft computing, modeling, optimization, statistical modeling, regression, swarm algorithm and machine learning. She can be contacted at email: nurezayana@uthm.edu.my.

Muhammad Ammar S.M. Shahrom pursued a master's degree in information technology at UTHM, focusing his research on soft computing techniques and artificial intelligence. In 2024, he worked as a System Analyst at Swift Integrated Logistics Sdn Bhd, located in Bandar Bukit Raja, Klang. During his tenure, he was responsible for managing projects related to the Warehouse Management System (WMS) and Freight Management System (FMS). He can be contacted at email: shafieammar79@gmail.com.

Mohamad Firdaus Ab. Aziz is a Senior Lecturer at the Faculty of Computer Science and Information Technology from Universiti Tun Hussein Onn Malaysia, Malaysia. He received her PhD in Computer Science from Universiti Teknologi Malaysia (UTM) in 2017 and his Master of Science (Computer Science) from the same university in 2007. His research interests include AI, machine learning, quantum based and classification in big datasets using AI algorithms. He can be contacted at email: mdfirdaus@uthm.edu.my.

Salama A. Mostafa received his B.Sc. in Computer Science from the University of Mosul, Iraq (2003), and M.Sc./Ph.D. in ICT from UNITEN, Malaysia (2011/2016). He is Managing Editor of the Journal of Soft Computing and Data Mining and former Head of CIAS, UTHM. Ranked among the World's Top 2% Scientists (Stanford/Elsevier, 2021–2025), he has published 229+ Scopus-indexed works with an H-index of 42. His expertise spans AI, machine learning, deep learning, optimization, and autonomous systems. He can be contacted at email: salama.adrees@alnoor.edu.iq.

Anis Farhan Kamaruzaman received her Bachelor of Science, Master of Computer Science, and Doctor of Philosophy in Computer Science from Universiti Teknologi Malaysia (UTM). Her research interests are in the areas of soft computing, modelling, optimization, statistical analysis, and swarm algorithms. She can be contacted at email: anisfarhankmi@yahoo.com.

Nor Bakiah Abd. Warif is a Senior Lecturer at Faculty of Computer Science & Information Technology, UTHM Previously, she was a Senior Lecturer at the Faculty of Computing, Universiti Malaysia Pahang. She received her Ph.D in Digital Forensics in 2018 from University of Malaya, Kuala Lumpur and a bachelor's degree in information technology at the National University of Malaysia, Bangi, Selangor. Her research interests are in the areas of image processing, digital forensics, deep learning, and object recognition. She can be contacted at email: norbakiah@uthm.edu.my.